

WRF DOWNSCALING EXPERIMENT OVER THE KERGUELEN ISLANDS

Ricardo Fonseca^{1,2}, Javier Martín-Torres^{1,3,4}

¹Group of Atmospheric Sciences, Luleå University of Technology, Sweden

²Khalifa University of Science and Technology, Abu Dhabi, United Arab Emirates

³Instituto Andaluz de Ciencias de la Tierra (CSIC-UGR), 18100 Granada, Spain

⁴The Pheasant Memorial Laboratory for Geochemistry and Cosmochemistry, Institute for Planetary Materials, Okayama University at Misasa, Japan

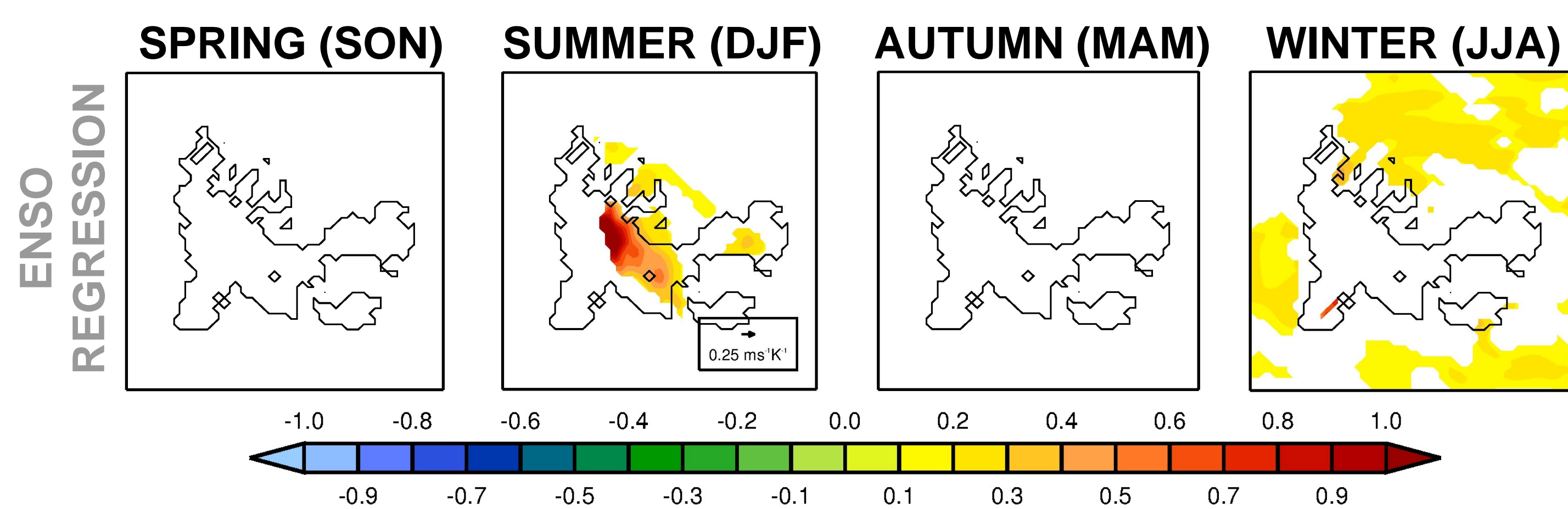


1. Introduction

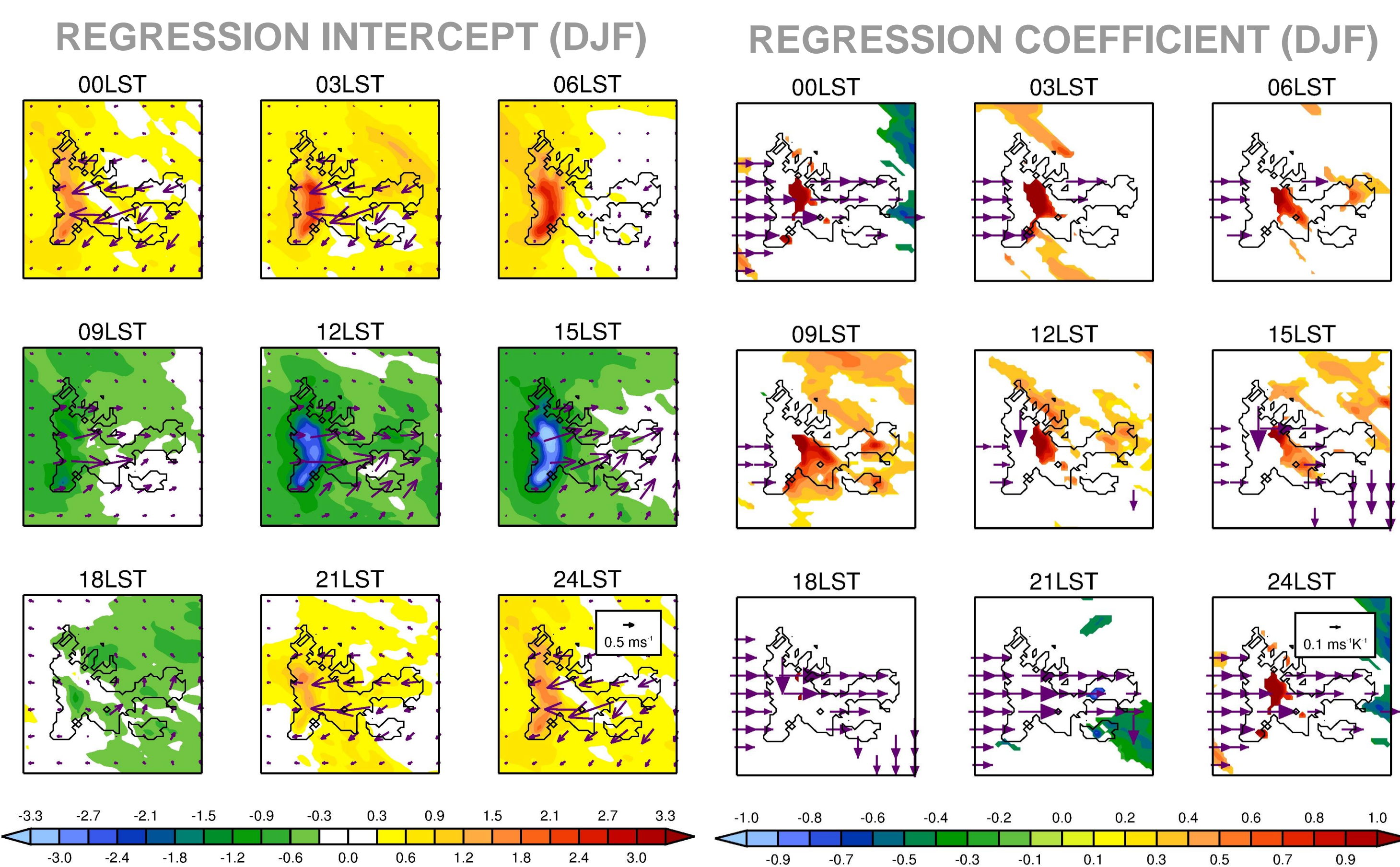
- Located in the southern Indian Ocean at about 49°S and 69°E, more than 3,300 km to the south-east of Madagascar, the Kerguelen (Desolation) Islands are one of the most remote places on Earth. Discovered by Yves-Joseph de Kerguelen-Trémarec in February 1772, the islands have an oceanic climate, with small daily and annual air temperature ranges and rather windy conditions (Varney, 1926).
- The Kerguelen Islands feature the Cook Ice Cap, a glacier located at relatively low altitude, and hence directly influenced by changes in the oceanic and atmospheric circulations (Verfaillie et al., 2015). Favier et al. (2016) showed that the glacier wastage in the islands during the 2000s was among the most dramatic on Earth. They also found that most of the climate models from the Coupled Model Intercomparison Project 5 (Taylor et al., 2012) do not simulate well the observed atmospheric conditions.
- General Circulation Models (GCMs) fail to reproduce the climate of the islands due to their coarse spatial resolution. Given the lack of high-resolution observational datasets over the region, a high-resolution simulation with a Regional Climate Model (RCM) that verifies well against the available observational data and extends over a considerable period of time is currently the best product that can be used to investigate the climate mean and variability of the Kerguelen Islands.

4. Regression Against ENSO Index

- In order to investigate the impact of El Niño – Southern Oscillation (ENSO) on the Kerguelen Islands, the monthly-mean precipitation rate and 10-meter horizontal wind vector are regressed against the ENSO index (Lestari and Koh, 2016) for each season. Below the regression coefficient of the precipitation rate (shading, units of $\text{mm day}^{-1} \text{K}^{-1}$) and 10-meter horizontal wind vector (arrows, units of $\text{ms}^{-1} \text{K}^{-1}$) are shown. Only regression coefficients statistically significant at 90% confidence level are plotted. For the wind vector, if the regression coefficients are only statistically significant for the zonal/meridional component, the arrow will point in the zonal/meridional direction with the arrowhead filled; if the two regression coefficients are statistically significant, the arrowhead is not filled.
- The regression coefficients for the precipitation are only statically significant in the solstitial seasons: in the austral winter (JJA) there is a general increase in precipitation during El Niño events, mostly over the oceans, whereas in the austral summer (DJF) the increase is mainly over land, and is more pronounced in the region just to the east of the Cook Ice Cap. While the higher amounts of rainfall over the oceans in JJA can be attributed to higher sea surface temperatures (Trenberth and Shea, 2005), there is no obvious explanation for what is causing the precipitation increase in DJF.



- One possibility is that the interaction with ENSO in this season occurs mainly through changes in the diurnal cycle. The figures below show the regression intercept and coefficient of the 3-hourly precipitation and 10-meter horizontal wind vector anomalies for DJF in Local Solar Time (LST).
- During the daytime, warmer temperatures on the low-land regions in the eastern and central parts of the island lead to lower pressures compared to those observed in the highlands to the west. The resulting westerly winds are in phase with the background winds, giving enhanced low-level divergence and drier conditions in particular in the Cook Ice Cap and in higher elevations of the Loranchet and Raillier du Baty Peninsulas. This pattern reverses in the evening and nighttime hours.
- The regression coefficient shows a persistent increase in rainfall in El Niño events more significant during nighttime and morning hours just to the east of the Cook Ice Cap, in the same region where the increase in the seasonal mean precipitation shown above is statistically significant. This results from the interaction between the anomalous circulation associated with ENSO with the local diurnal cycle: convergence of the easterly diurnal cycle winds with the anomalous westerly winds in El Niño events at night, and with the anomalous northerly winds during morning hours.



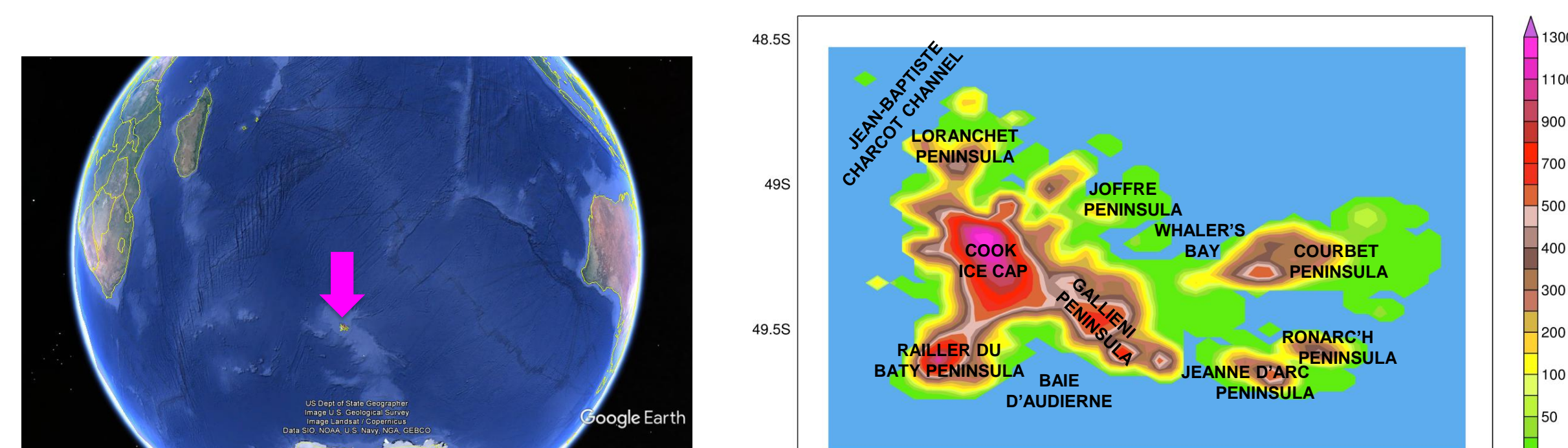
2. Regional Atmospheric Climate Model

In this study the Weather Research and Forecasting model version 3.7.1 (WRF; Skamarok et al., 2008) is used to dynamically downscale 30 years (April 1986 – March 2016) of the $0.5^\circ \times 0.5^\circ$ (~55 km) National Centers for Environmental Prediction Climate Forecast System Reanalysis (CFRS; Saha et al., 2010) over the Kerguelen Islands. WRF is run in a three-nested configuration (resolutions of 27, 9 and 3 km) with 40 levels in the vertical, concentrated in the Planetary Boundary Layer (PBL). The output of the 3 km grid is first post-processed, stored every 1 h, and subsequently used for analysis. Further details about the experimental setup are given in Fonseca and Martín-Torres (2018).

The physics parameterization schemes employed are shown in the table below:

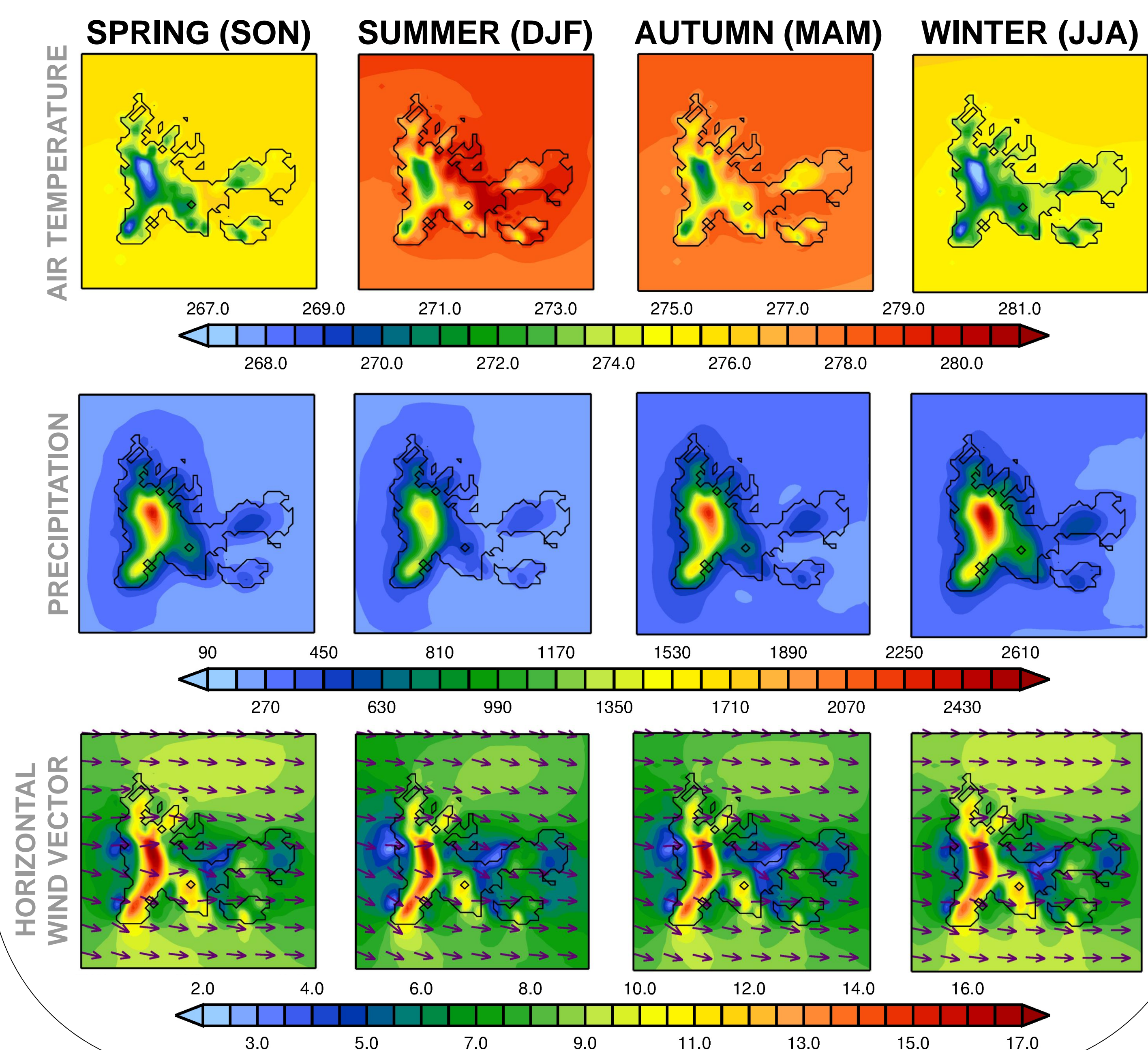
Physics Options	Parameterization Scheme
Microphysics	Goddard (six-class) Cloud Microphysics Scheme
Radiation	Rapid Radiative Transfer Model for GCM Applications (RRTMG)
Surface Layer	Revised MM5 Monin-Obukhov Scheme
Land Surface	Noah Land Surface Model
Planetary Boundary Layer	Mellor-Yamada Nakanishi and Niino (MYNN) Level 2.5
Cumulus (27 km and 9 km grids only)	Betts-Miller-Janjić (BMJ) Scheme + Precipitating Convective Cloud (PCC) Scheme (Koh et al., 2016)
Sea Surface Temperature	CFRS SST + simple skin temperature scheme (Zeng et al., 2005)

The figure on the left (taken from Google Earth) gives the location of the Kerguelen Islands and the one on the right shows the spatial extent (with boundary regions excluded) and orography (m) of the 3 km model domain. The different regions of the Kerguelen Islands are labelled.



3. Seasonal Mean Climate

- Below the 2-meter air temperature (K), precipitation (mm) and 10-meter horizontal wind (the arrows show the direction and the shading the speed in m s^{-1}) averaged over the 30-year period is shown for each season: austral spring (September to November, SON), summer (December to February, DJF), autumn (March to May, MAM) and winter (June to August, JJA).
- As expected, over the high terrain the seasonal mean temperatures are lower, with the 0°C isotherm around the Cook Ice Cap in JJA. The highest seasonal mean temperatures, around 282 K (8.85°C), occur in DJF in the low elevations between the Gallieni and Courbet Peninsulas whereas the lowest temperatures of about 266 K (-7.15°C) are found in the Cook Ice Cap in the winter season. Over the surrounding oceans, the annual temperature variability is smaller, with typical values of 275 K in winter and 278 K in the summer.
- In line with Favier et al. (2016), WRF shows a significant correlation between precipitation and elevation. The heaviest precipitation of ~2700 mm are predicted at the highest elevations of the Cook Ice Cap in winter. The eastern side of the Courbet Peninsula and the lower elevations between the Courbet and Gallieni Peninsulas that experience the warmest seasonal mean temperatures generally have the lowest total amount of precipitation for all seasons.
- The strongest westerly/north-westerly winds occur over high terrain, mostly in a banded region that extends from the northern section of the Loranchet Peninsula to the southern section of the Raillier du Baty Peninsula, comprising the Cook Ice Cap, with seasonal mean values in excess of 17 m s^{-1} . The most wind-sheltered areas are the southeastern parts of the Courbet Peninsula, and the region between the Gallieni and Courbet Peninsulas mainly along the northwestern coastline facing the Whaler's Bay, where the wind speeds are generally less than 6 m s^{-1} .



References

- Favier, V. and Coauthors, 2016: Atmospheric drying as the main driver of dramatic glacier wastage in the southern Indian Ocean. *Sci. Rep.*, 6:32396, doi:10.1038/srep32396.
- Fonseca, R. M., Martín-Torres, J. M., 2018: High-resolution dynamical downscaling of re-analysis data over the Kerguelen Islands using the WRF model. *Theor. Appl. Climatol.*, 135, 1259-1277.
- Koh, T.Y. and R.M. Fonseca, 2016: Subgrid-scale Cloud-Radiation Feedback For the Betts-Miller-Janjić Convection Scheme. *Q. J. R. Meteorol. Soc.*, 142, 989-1006.
- Lestari, R. K. and T.-Y. Koh, 2016: Statistical Evidence for Asymmetry in ENSO-IOD Interactions. *Atmos.-Ocean*, 54, 498-504.
- Saha, S. and Coauthors, 2010: The NCEP Climate Forecast System Reanalysis. *Bull. Amer. Meteorol. Soc.*, 91, 1015-1057.
- Skamarock, W. C. and Coauthors, 2008: A description of the Advanced Research WRF version 3. NCAR tech. Note TN-475, STR, 113pp.
- Taylor, K.E. and Coauthors, 2012: An Overview of the CMIP5 and the Experiment Design. *Bull. Am. Meteorol. Soc.*, 93, 485-498.
- Trenberth, K.E. and D.J. Shea, 2005: Relationships between precipitation and sea surface temperature. *Geophys. Res. Lett.*, 32:L14703, doi: 10.1029/2005GL022760.
- Varney, B. M., 1926: Climate and Weather at Kerguelen Islands. *Mon. Wea. Rev.*, 54, 425-426.
- Verfaillie, D. and Coauthors, 2015: Recent glacier decline in the Kerguelen Islands (49°S, 69°E) derived from modelling, field observations and satellite data. *J. Geophys. Res. Earth Surf.*, 120, 637-654.
- Zeng, X. and Beljaars, A., 2005: A prognostic scheme of sea surface skin temperature for modeling and data assimilation. *Geophys. Res. Lett.*, 32:L14605, doi:10.1029/2005GL023030.